Investigation on the Characteristics of Internal Flow within Three-Dimensional Axial Pump Based on Different Flow Conditions

Ahmed Ramadhan Al-Obaidi[1], Hussam Ali Khalaf[2], Jassim Alhamid[3]

{ahmedram@uomustansiriyah.edu.iq}

[1]Department of Mechanical Engineering, College of Engineering, Mustansiriyah University, Baghdad, Iraq
[2]Department of Mechanical Engineering, College of Engineering, University of Thi-Qar, Iraq
[3]Washington State University, School of Mechanical and Materials Engineering, WSU Tri-Cities, USA

Abstract. In order to make the axial pump has improved performance, it is important to distinguish regarding the flowing distributions. According to the Navier–Stokes equations (NSE), Standard k − ϵ turbulence model and algorithm of SIMPLE, the CFD technique investigation is applied of the three dimensions flow passage in pump using the sliding mesh approach (SMA). The structural of numerical unsteady flow simulation and behaviour transient dynamic study of an axial pump is carried out at various conditions depend on the method of fluid-structure interaction. Numerical outcomes reveal that the higher-pressure distribution of axial impeller happens at the outer impeller diameter closed to the tip blade region and the impeller hub. Also, the higher velocity occurs near later regions. The analysis result reveals the study of flow field in the pump can provide a good guide for the axial pump designing as well as the producing practice. The velocity increases as the flow reaches to the tip blade region. Then it is decreases as the flow far away from the tip region. This is due to the high interaction flow in this area between the flow and the tip blade. Moreover, based on the numerical outcomes, it was noted that the tip blade has the high effect on the flow pattern and performance of the axial pump.

Keywords: Characteristics of Internal Flow, Three-Dimensional Axial Flow Pump, Different Conditions, Numerical analysis

1. Introduction

Axial-flow pumps are a type of dynamic pump that offers wide adaptability and is used in a broad range of applications due to its simple structure, easy installation and maintenance, small engineering investment, and stable operation [1, 2]. In recent years, as the use of axial-flow pumps has become more widespread, there has been increasing focus on enhancing efficiency, safety, and stability [3-5]. Using similar operating conditions, Shi Lijian et al. [6] studied how main design parameters influenced pump performance. Axial-flow pumps were designed according to the direction in which blade performance changes. Following the modification of design parameters, the researchers performed a numerical analysis using CFD to determine the final modified design scheme for the axial-flow pump. An axial pump impeller blade was studied by Manjunatha and Nataraj [7] under similar operating conditions.

ICONSEIR 2022, November 24, Medan, Indonesia

DOI 10.4108/eai.24-11-2022.2332720

Upon comparing the numerical simulation results of the pump's performance with the experimental data, they discovered that the axial direction on the discharge side of the impeller experiences high pressure. The researchers also noted the occurrence of high recirculation flow near the blade suction side at low flow rates, which diminished as the flow rate increased in that region. Additionally, various investigations have been carried out on the performance of axial flow pumps, including the work done by Momosaki et al. [8], who utilized computational fluid dynamics (CFD) to conduct a numerical simulation of the internal flow in an axial flow pump under partial flow rate and design flow rate conditions.

In order to test an axial pump, the researchers designed a test rig with specific parameters: a flow rate of 70 L/s, a head of 4.0 m, and an impeller speed of 1225 rpm. A comparison of unsteady flow simulation results with experimental results revealed that the simulation accurately predicted pump performance.

At low flow rates, the fluid flowed smoothly near the rear rotor blade's leading edge at the suction surface. However, a strong tip vortex leakage occurred close to the leading blade edge. In addition, flow separation occurred downstream mid-chord on the suction surface, near the hub to the mid-span region. Flow patterns in some vanes indicated an axially long and compact radial profile, whereas mixed flows in part volutes displayed vertically reliable and robust pancake profiles. Moreover, the axial rotor displayed good performance as a pump under the designed operating conditions. Additionally, mixed flow impellers exhibit better suction performance under design conditions and exhibit a larger region of maximum efficiency. In an axial-flow pump, Zhu et al. [10] examined the evolution of unsteady flow during transient conditions to investigate the mechanism of transient flow formation. The study revealed that velocity and pressure increased linearly with time initially and then stabilized once the rotating speed reached a steady state.

The use of three-dimensional numerical simulations based on computational fluid dynamics (CFD) has been a crucial method for predicting the internal flow characteristics of axial flow pumps under various conditions. A 3D numerical simulation of unsteady turbulent flow in axial-flow pumps was conducted by Zhang et al. [11]. The numerical findings indicated that the unsteady prediction results were more precise than the steady results, and the study also examined the static pressure fluctuation.

Tao et al. [12] examined the hydrodynamics of sweep blades in a high-speed axial fuel pump impeller. The study investigated three types of hydrodynamic performance: straight, positive, and negative axial sweep blades in fuel pumps through the use of three modeled impellers. The impellers had an outside diameter of 70mm and four blades, and the pump's rotational speed was 8000 rpm, with a mass flow rate of 10.75 kg/s. The study's results revealed that vortex flow occurred near the inlet blade surface, increasing in intensity towards the tip blade area. A positive sweep blade reduces hydraulic flow losses and operates in an unstable operating zone due to stalled fluid in the middle part of the impeller blade. Axial fuel pumps using this blade type will also be more secure and stable. A full tubular and axial-flow pump was simulated and validated using numerical simulations and model test research methods.

Numerical unsteady flow simulation and behavior transient dynamic studies of an axial pump were conducted at various conditions, utilizing the fluid-structure interaction method. The numerical results revealed that higher pressure distribution occurred at the outer impeller diameter close to the tip blade region and impeller hub, while higher velocity occurred in later areas. These findings suggest that analyzing the flow field in the pump can offer a valuable guide for designing and producing axial pumps.

2. Computational Method and Physical Model

2.1 Physical Model Description

The physical flow domain model of axial pump is depicted in Figure 1. This figure illustrates the 3D flow computational domain which involves of segment of pump, inlet flow and outlet flow pipes. The pump geometrical parameters consist of a 4-blade impeller, the impeller diameter is 101 mm, the blade tip clearance gap is 1 mm and the impeller Hub diameter is 50 mm, the impeller speed of 3000 rpm and the design flow rate is 12.5 l/min.

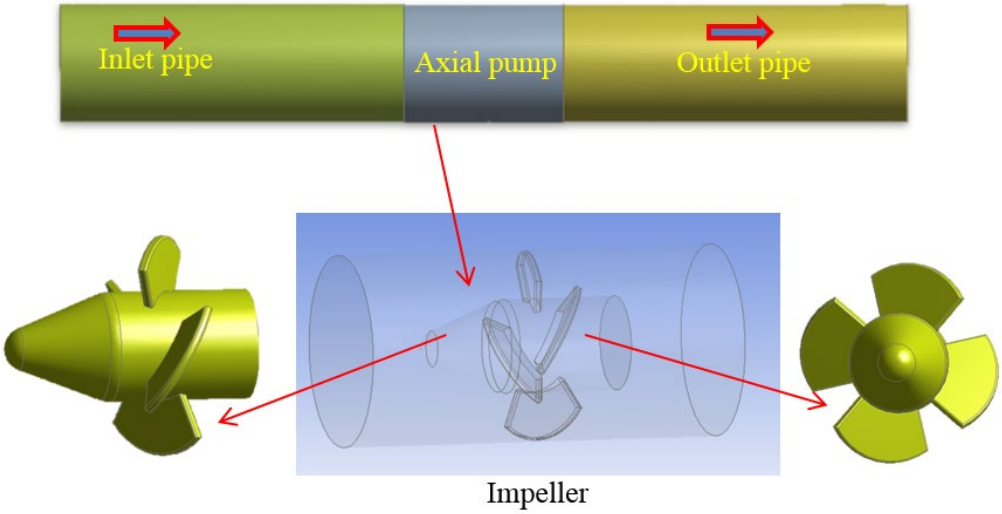

Fig. 1. Axial pump physical model

2.1 Mesh Flow Generation

The fluid computational wall grid regions and unstructured mesh of the pump consist of inlet pipe, impeller and outlet pipe are represented in Figure 2. For efficiently control the grid distribution in the pump model, the entire tetrahedral grid strategy is used. The flow numerical model in this investigation is divided into three domains. Hence, each part is linked through the interfaces part that are set at a inlet region and outlet region of the pump impeller. The mesh is generated for all pump parts through the use of ANSYS ICEM CFD software. Hence, the distribution of mesh cell number is guaranteed reliably at the interface transition regions. To obtain good result the mesh independent analysis simulation is carried out with different grid topology and distribution of the pump model. The interface connection between all parts and the general grid interface are used in order to the grid on either part sides are connected surfaces and permits matching. For the characteristics of transient flow simulation in the pump the model of rotor stator interface is applied which in order to permit the smooth rotation flow between the components.

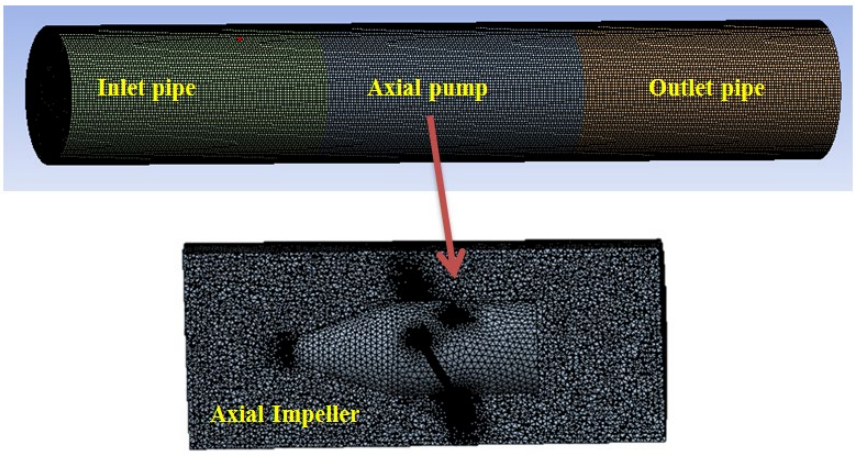

Fig. 2. mesh flow generation for axial pump and all parts

2.2 Computational Simulation Approach

By using computational software of Fluent, the 3D numerical model of the axial pump is created, including different parts namely: inlet straight pipe, impeller axial pump and outlet straight pipe. The CFD Fluent is applied to model the internal flow behaviour of the pump. In this work, the Reynolds time-averaged viscous Navier-Stokes equations (RTAVNSE) are adopted to numerical simulate the internal 3D flows, using the standard κ-ε turbulence model. Applying N-S equation for this type of pump,

$$\frac{\partial(\rho u_i)}{\partial x_i} = 0 \tag{1}$$

$$\frac{\partial(\rho u_i u_j)}{\partial x_i} = -\frac{\partial p}{\partial x_i} + \frac{\partial\left[\mu_e\left(\frac{\partial u_i}{\partial x_j} + \frac{\partial u_j}{\partial x_i}\right)\right]}{\partial x_j} - 2\ \varepsilon_{ijk} k \omega_j u_k \tag{2}$$

Where P is the fluid pressure, ε_{ijk} is the fluid stress tensors, ρ fluid density, μ is viscosity and $u_i, u_j,$ are the mean velocity components. To close the N-S equation, k- ε turbulence model has been employed, below the transport equations for this pump model

$$\mu_e = \mu + \mu_t \tag{3}$$

$$\mu_t = \rho c_\mu k^2 / \varepsilon \tag{4}$$

$$\frac{\partial}{\partial x_j} = \left[\rho u_j k - \left(\mu + \frac{\mu_t}{\sigma_k}\right)\frac{\partial k}{\partial x_j}\right] = \rho(P_k - \varepsilon) \tag{5}$$

$$\frac{\partial}{\partial x_j} = \left[\rho u_j \varepsilon - \left(\mu + \frac{\mu_t}{\sigma_t}\right)\frac{\partial \varepsilon}{\partial x_j}\right] = \rho\ \frac{\varepsilon}{k}(C_1 P_k - C_2 \varepsilon) \tag{6}$$

$$P_k = \frac{\mu_t}{\rho}\left(\frac{\partial u_i}{\partial x_j} + \frac{\partial u_j}{\partial x_i}\right)\frac{\partial u_i}{\partial x_j} \tag{7}$$

$$C_\mu = 0.09\,, C_1 = 1.44, C_2 = 1.92, \sigma_k = 1.0. \sigma_\varepsilon = 1.3 \tag{8}$$

2.3 Boundary Flow Conditions

In this research, the boundary flow conditions comprise inlet velocity at the inlet section. outlet pressure along the axial flow direction is specified at the outlet section [13-15]. Also, at the inlet the standard atmospheric pressure is given. Flow field in a axial impeller is solved and computed using sliding mesh analysis (SMA), whereas the flow in the inlet and outlet pipes are computed as the stationary parts. The algorithm type SIMPLEC is applied to couple pressure and velocity to increase the computation efficiency. The quality of mesh for the pump is checked and the mesh independence calculations sizes are carried out before start the numerical calculations formally commenced.

3 Results and Discussion

3.1 Validation of the Numerical Model

The curves of hydrodynamic performance comparison between experimental [16] and numerical approaches under various conditions flow is represented in Figure 3. As noticed that from this figure, compared with the standard k - ϵ model, numerical outcomes by using SIMPLEC algorithm and couple pressure and velocity model are provided better agreement results as compared to the experimental data at the different load boundary condition. Besides, the relative errors for both results maintain is lower than 7%.

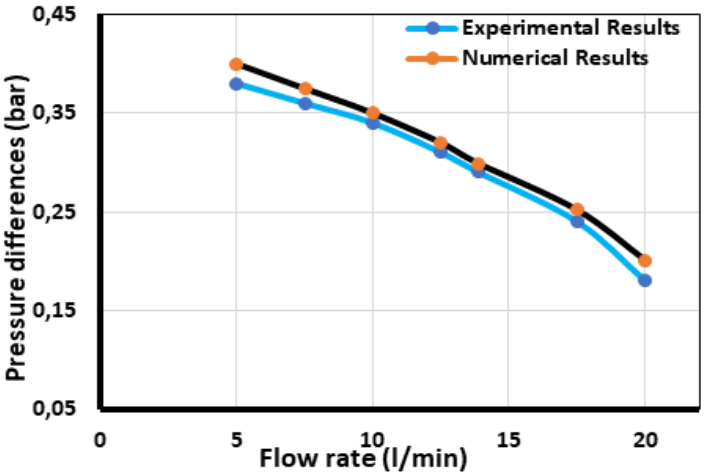

Fig. 3. Comparison between experimental and numerical data

3.2 Characterises of Hydraulic Performance

In this part, the analysis of pressure distribution comparative analysis as described in Figure 4. As show in this figure the pressure distribution is located centre pump sections under various pump mass flows. It can be noted that the pressure gradually increases form the inlet impeller diameter to outlet and the maximum pressure occurs near the tip clearance of blade passage. Also, the pressure at the discharge region is higher than the section part for all cases. Owing to the action of tip clearance, the pressure in the flow passage seems as clear variations in this area. As the flow rate decreases to 20 l/min, the pressure distribution becomes more obvious. The pressure in the tip clearance area is higher than that in the other pump area. Indicating that tip clearance has a important effect on the distribution in pressure in the flow impeller passage under different conditions. Therefore, investigation the effect of tip clearance size on flow field in the in-blade passage of the pump such as pressure distribution has significant influence on the pum performance.

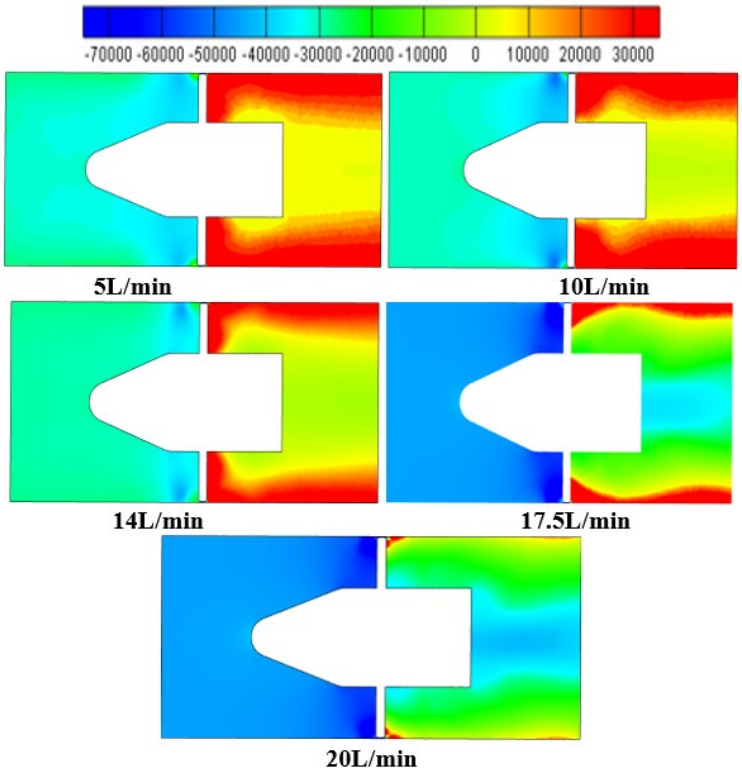

Fig. 4. Pressure variations contours for various cases

Figure 5 displays the pressure distribution in the radial impeller at different section regions and with various conditions from 5 to 20 l/min. The contours of the pressure is showed in different sections, corresponding to the flow direction in the pump, as revealed in this figure. As observed in the tip blade area, the internal pressure in the pump is much higher than that of the other surrounding impeller regions. For the flow rate of 5 l/min, the internal pressure increases gradually, and the size of high pressure region increases accordingly when

the flow rate decreases particularly near the tip blade edge region. This happened due to increase the size of the vortex flow region continuously.

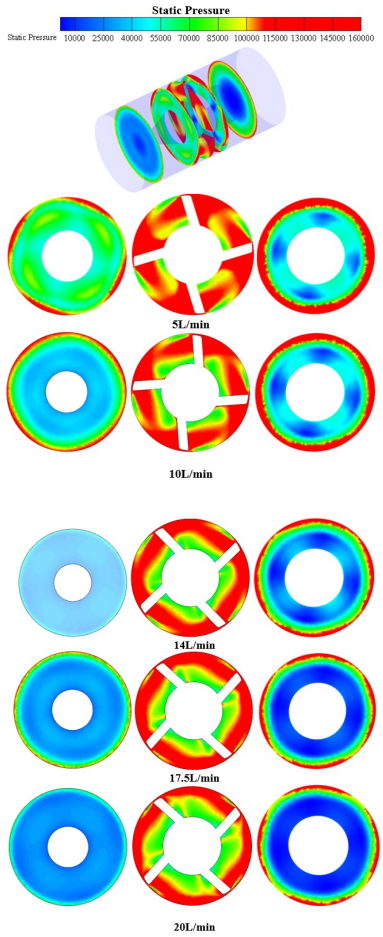

Fig. 5. Pressure variations contours at various cases and locations in the pump

For more analysis, in order to understand the complex flow structure in the pump, the static pressure, and velocity magnitude are chosen to quantitative analyse purpose. It is noteworthy that these parameters graphs in this numerical investigation are plotted along with the flow direction with straight analysis red line passed through an axial pump as demonstrated in Figure 6.

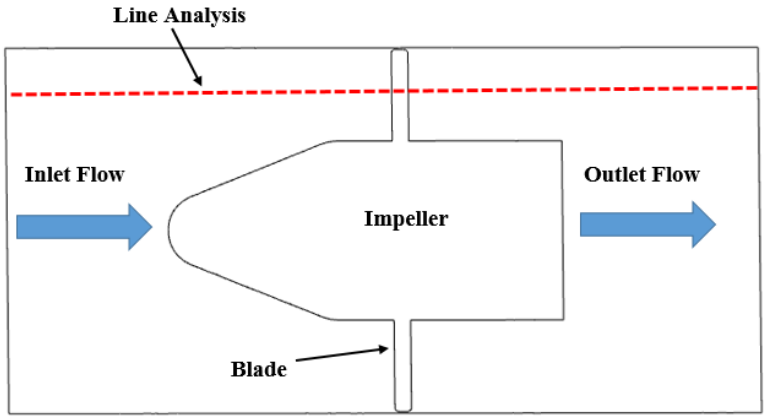

Fig. 6. Line analysis across the axial pump

Figure 7 illustrates the pressure distributions across the pump by using line analysis under different flow rate conditions. As seen from this figure the pressure gradually decreases as the flow rate increases. The higher value of pressure takes place near the tip blade region for all cases as expected. As observed form this Figure the pressure variance between the discharge sides in impeller is higher than suction side, and higher pressure occurs basically closed the tip blade area.

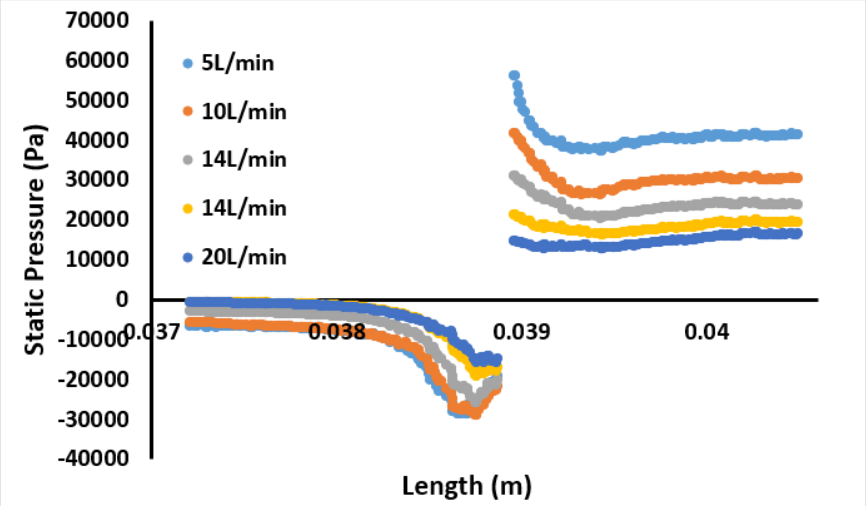

Fig. 7. Distribution of static pressure in axial flow direction

Figure 8 represents the velocity distributions under varying flow cases. As observed that on the suction and discharge pump sides the internal velocity change with flow rate changes and the velocity at the inlet and outlet impeller hub region have the minimum velocity distributions. However, the velocity slightly over the impeller hub. On the tip blade section velocity has the maximum value due to the vortex size and secondary flow increases sharply in this region and the vortex area is more than that with another region in the pump. With the decrease of the flow rate, the vortex size flow and secondary flow in tip regions are increased.

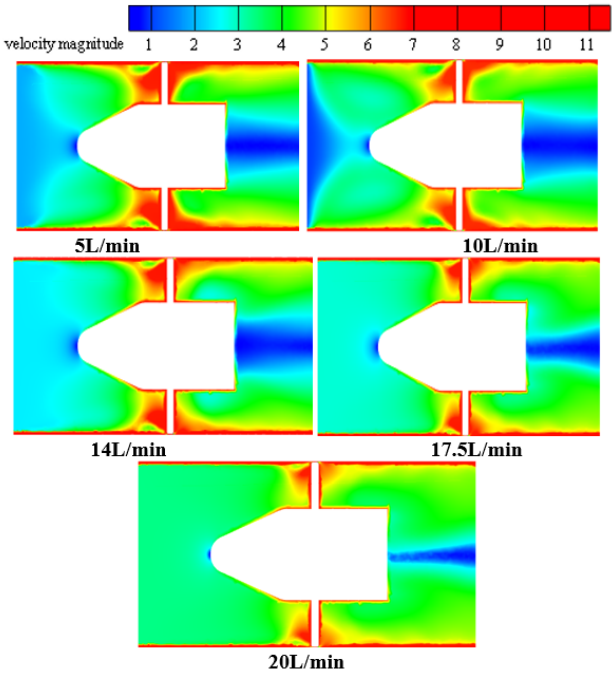

Fig. 8. Velocity distributions under varying flow cases

For quantitative analysis, Figure 9 describes the velocity variations across the axial impeller pump. As noted from this figure the velocity increases as the flow reaches to the tip blade region. Then it is decreases as the flow far away from the tip region. This is due to the high interaction flow in this area between the flow and the tip blade. This interaction can lead to increase the vortex and secondary flow near this area.

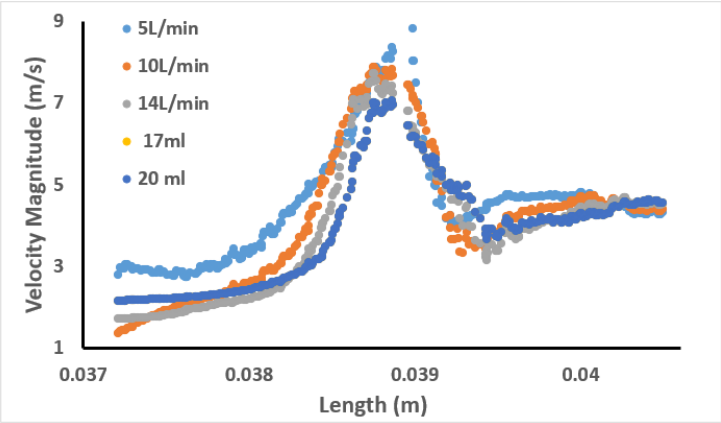

Fig. 9. Distribution of velocity magnitude in axial flow direction

4 Conclusion

By investigating the flow field rule such as the velocity and pressure distribution in an axial pump. Distribution around the pressure and velocity inside the pump is irregular. The outcomes of this work are reliable with the expected characteristics of flow in axial pump, representing that the numerical models can apply to evaluate the performance of axial pump in design environment. Based on above analysis it can be observed following results:

a. The numerical pump pressure revealed a good agreement as compared to the experimental available results.
b. Different flow behaviours in the pump under various flow rates were obtained by numerical model.
c. The pressure gradually increases form the inlet impeller diameter to outlet and the maximum pressure occurs near the tip clearance of blade passage. Also, the pressure at the discharge region is higher than the section part for all cases.
d. For the flow rate of 5 l/min, the internal pressure increases gradually, and the size of high pressure region increases accordingly when the flow rate decreases particularly near the tip blade edge region.
e. The pressure variance between the discharge side in impeller is higher than suction side, and higher pressure occurs basically closed the tip blade area.
f. The internal velocity change with flow rate changes and the velocity at the inlet and outlet impeller hub region have the minimum velocity distributions.
g. The velocity increases as the flow reaches to the tip blade region. Then it is decreases as the flow far away from the tip region. This is due to the high interaction flow in this area between the flow and the tip blade.
h. Based on the numerical outcomes, it was noted that the tip blade has the high effect on the flow pattern and performance of the axial pump.

Acknowledgments

In this recent research work, the authors wish to acknowledge more both the Mustansiriyah University Baghdad – Iraq (www.uomustansiriyah.edu.iq) and Washington State University, Washington, the USA, for their support.

Author ORCID ID

Asst. Prof. Dr. Ahmed Ramadhan Al-Obaidi
https://orcid.org/0000-0003-3819-7008

References

[1] Brennen, C. E. (2012, November). A review of the dynamics of cavitating pumps. In IOP Conference Series: Earth and Environmental Science (Vol. 15, No. 1, p. 012001). IOP Publishing.

[2] Al-Obaidi, A. R. (2020). Experimental comparative investigations to evaluate cavitation conditions within a centrifugal pump based on vibration and acoustic analyses techniques. Archives of Acoustics, 45(3), 541-556.
[3] Al-Obaidi, A. R. (2020). Influence of guide vanes on the flow fields and performance of axial pump under unsteady flow conditions: Numerical study. Journal of Mechanical Engineering and Sciences, 14(2), 6570-6593.
[4] Li, D., Wang, H., Li, Z., Nielsen, T. K., Goyal, R., Wei, X., & Qin, D. (2018). Transient characteristics during the closure of guide vanes in a pump-turbine in pump mode. Renewable Energy, 118, 973-983.
[5] Al-Obaidi, A. R. (2020). Experimental investigation of cavitation characteristics within a centrifugal pump based on acoustic analysis technique. International Journal of Fluid Mechanics Research, 47(6).
[6] Shi, L., Tang, F., Xie, R., Qi, L., & Yang, Z. (2015). Design of axial flow pump modification and its effect based on CFD calculation. Transactions of the Chinese Society of Agricultural Engineering, 31(4), 97-102.
[7] Al-Obaidi, A. R. (2019, July). Numerical investigation of flow field behaviour and pressure fluctuations within an axial flow pump under transient flow pattern based on CFD analysis method. In Journal of Physics: Conference Series (Vol. 1279, No. 1, p. 012069). IOP Publishing.
[8] Momosaki, S., Usami, S., Watanabe, S., & Furukawa, A. (2010, August). Numerical simulation of internal flow in a contra-rotating axial flow pump. In IOP conference series: Earth and environmental science (Vol. 12, No. 1, p. 012046). IOP Publishing.
[9] Pan, Z., Ni, Y., Yuan, J., & Ji, P. (2015, November). Hydraulic Performance Comparison for Axial Flow Impeller and Mixed Flow Impeller with Same Specific Speed. In Journal of Physics: Conference Series (Vol. 656, No. 1, p. 012068). IOP Publishing.
[10] ZHU, Z., GUO, X., & CUI, B. (2011). External characteristics and internal flow features of a centrifugal pump during rapid startup [J]. Chinese Journal of Mechanical Engineering, 24(5), 798-804.
[11] Zhang, D. S., Shi, W. D., Bin, C., & Guan, X. F. (2010). Unsteady flow analysis and experimental investigation of axial-flow pump. Journal of Hydrodynamics, Ser. B, 22(1), 35-43.
[12] Tao, R., Xiao, R., Yang, W., Wang, F., & Wu, Y. (2013). Investigation of the hydrodynamics of sweep blade in hi-speed axial fuel pump impeller. Advances in Mechanical Engineering, 5, 174017.
[13] Al-Obaidi, A. R. (2021). Numerical investigation on effect of various pump rotational speeds on performance of centrifugal pump based on CFD analysis technique. International Journal of Modeling, Simulation, and Scientific Computing, 2150045.
[14] Al-Obaidi, A. R., & Alhamid, J. (2021). Numerical investigation of fluid flow, characteristics of thermal performance and enhancement of heat transfer of corrugated pipes with various configurations. In Journal of Physics: Conference Series (Vol. 1733, No. 1, p. 012004). IOP Publishing.
[15] Al-Obaidi, A. R., & Chaer, I. (2021). Study of the flow characteristics, pressure drop and augmentation of heat performance in a horizontal pipe with and without twisted tape inserts. Case Studies in Thermal Engineering, 25, 100964.
[16] Mostafa, N. H., & Mohamed, A. (2012). Effect of blade angle on cavitation phenomenon in axial pump. Journal of Applied Mechanical Engineering, 3(1), 1-6.